AC coupling losses in CICCs: analytical modeling at different stages

Alexandre Louzguiti, Louis Zani, Daniel Ciazynski, Bernard Turck, Jean-Luc Duchateau, Alexandre Torre, Frederic Topin

AC coupling losses in CICCs: analytical modeling at different stages

A. Louzguiti, L. Zani, D. Ciazynski, B. Turck, JL. Duchateau, A. Torre and F. Topin

***Abstract*—Cable-in-conduit conductors (CICCs) are composed of a large number of strands (superconducting composites and copper strands) twisted together in several stages with different twist pitches. They are widely used in large fusion tokamaks such as JT-60SA or ITER. However, because of their complex transposed geometry at strand scale, the knowledge of AC coupling losses in these conductors is limited and still has some improvement margins to capture its complexity while the prediction of their behavior under transient regimes (e.g. central solenoid) is of first importance to assess a safe operation in tokamaks. Consequently, we have carried out an in-depth theoretical generic study of a single stage of a CICC and analytically derived the expression of coupling losses using physical parameters (time constant and partial shielding coefficient) determined from electromagnetic and geometrical properties. Our approach has been inspired by the MPAS model (extensively used on the experimental ITER database) but starts from the analytical description of a single stage and aims at reaching the CICC scale in an iterative way.**

***Index Terms*—AC losses, analytical, superconducting, transient regimes**

I. Introduction

A common way [1]–[5] to model coupling losses occurring in a superconducting multifilamentary composite subject to a transverse and uniform time-varying magnetic field is to use the equation

$$B_{int} + \tau \dot{B}_{int} = B_a \tag{1}$$

which quantifies the local uniform induction B_{int} inside the composite as a function of the uniform external magnetic excitation B_a and of the time constant τ of the coupling currents.

The computation of the instant power dissipated by AC coupling currents per unit volume of composite leads to the following expression

$$P = 2\tau \dot{B}_{int}{}^2/\mu_0 \tag{2}$$

It has been shown [1]–[3] that the single time constant approach above is valid for any cylindrical composites with a central filamentary zone under any magnetic excitation regime. This approach still holds for composites with more complex design and even for CICCs provided that the magnetic excitation variation is slow compared to the largest time constant of the system (e.g. for the TFJS1 conductor, under $f = 0.2\,Hz$ $(5\,s)$ the discrepancy between the experimental data [6] and the single time constant approach using $n\tau = 62\,ms$ is lower than 10%, which is consistent with the fact that $5\,s \gg 62\,ms$).

However, when the condition of slow variation is not fulfilled, the single time constant approach is no longer sufficient to describe the system response as depicted in [7]–[12]. After several studies [7], [9], [11], [13], the Multizone Partial Shielding (MPAS) model [6] offers another analytical perspective to treat these cases by assigning a basic time constant to each cabling stage of a CICC. Our philosophy, inspired by the MPAS model, is based on the fact that the response of every stage of a cable to a magnetic excitation can be represented by a magnetic dipole partially screening the external field variation. Therefore, the instant power density in each isolated stage j would be in average

$$P_j = nk_j \tau_j \dot{B}_{int\,j}{}^2/\mu_0 \tag{3}$$

where τ_j is the time constant of the coupling currents and nk_j the partial magnetic shielding coefficient of stage j, $B_{int\,j}$ being the uniform internal induction governed by (1) inside stage j.

However in a cable there exists some coupling between each stage so that the time constants τ_j do not correspond to the global time constants of the cable. The cable is in fact governed by a matrix equation whose vectors are the coupling currents of each stage and whose matrix coefficients are analogous to time constants. Using the eigenbasis, new time constants Θ_j (eigenvalues of the matrix) can be found to express the total coupling losses as a sum of terms similar to (3). As a result, and according to several experimental results [9], [6], the total instant power density due to AC coupling losses in a cable with N time constants (strand counted as one stage) can be expressed, as in the MPAS model, as

$$P = \sum_{j=1}^{N} n\alpha_j \Theta_j \dot{B}_{int\,j}{}^2/\mu_0 \tag{4}$$

the $n\alpha_j$ are the equivalent to the nk_j in the eigenbasis.

The MPAS model looks to be a very useful analytical tool to characterize a conductor response to an external magnetic variation as it is being extensively used on ITER conductors but has to be adjusted on experimental classical curves.

Manuscript submitted for review September 6, 2016.

This work was supported in part by the Conseil Régional Provence-Alpes-Côte d'Azur and by ASSYSTEM.

A. Louzguiti (corresponding author phone: +33442254749; e-mail: alexandre.louzguiti@cea.fr), L. Zani, D. Ciazynski, B. Turck, JL. Duchateau and A.Torre are with Commissariat à l'Energie Atomique et aux Energies Alternatives, CEA/DSM/IRFM, CEA Cadarache 13108 St Paul-Lez-Durance, France.

A. Louzguiti is also with Aix Marseille Université, CNRS, IUSTI UMR 7343, 13453, Marseille, France together with F. Topin.

Contrary to this model, our main long term objective is to provide the analytical expressions of $n\alpha_j$ and Θ_j using only the electrical and geometrical parameters of a cable. This would lead us to a predictive model of AC coupling losses in CICCs. In order to do so, we first need to compute the nk_j and τ_j values of each isolated stage. The purpose of the present contribution is therefore to derive these expressions.

II. Analytical Modeling of a Single Stage

We first derive the electromagnetic equations governing the first cabling stage (i.e. a group of composites). Nevertheless it is important to note that we will not describe the whole first cabling stage, meaning that we will consider only the coupling currents circulating from one strand to another without taking into account the ones flowing within each strand. In doing so we will obtain the behavior of a single stage as we consider that the currents inside the composite are due to the shielding by the strand stage (i.e. by filaments).

A. Assumptions

The strands (of radius R) present in the considered N-uplet (i.e. group of N strands) are composed of

superconductor core (of radius R_f) surrounded by a copper shell and are numbered clockwise from $k = 1$ to N on Fig. 1. The external magnetic field B_a is assumed transverse (along the y-axis, see Fig. 1) and spatially uniform within the N-uplet. The strands are unsaturated (i.e. $\vec{E} = \vec{0}$ in the middle of each strand). Moreover, we consider $\left(2\pi R_c/l_p\right)^2 \ll 1$ where R_c is the twisting radius and l_p the twist pitch (i.e. a lightly twisted bundle). B_a temporal changes are slow enough to neglect displacement current so that $\vec{\nabla}.\vec{\jmath} = 0$ where $\vec{\jmath}$ is the current density inside the N-uplet, and to neglect the magnetic field generated by the currents flowing through the resistive parts of the N-uplet since its dimensions are small enough. The equivalent cross-section resistivity between the centers of adjacent strands is noted $\rho_t = \rho_b e_b/R$ and is mostly due to the contact zone (of width l_c, resistivity ρ_b and thickness $2e_b \ll R$, see Fig. 1). This contact is considered continuous, identical between every strand and without any deformation of the strands so that $R_c = R/\sin(\pi/N)$.

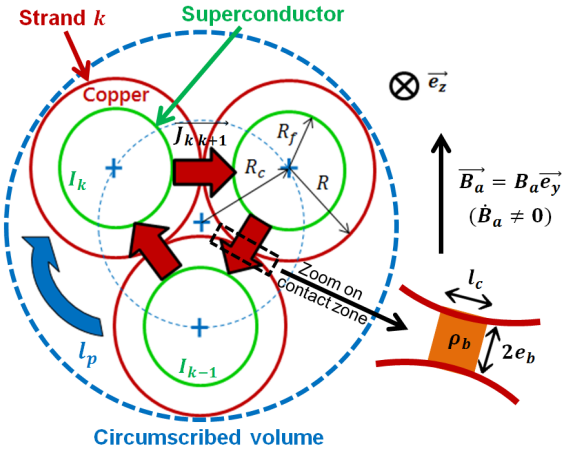

Fig. 1. Scheme showing the cross-section geometry of a triplet (N =3)

B. N-uplet model

Although all the calculations will not be presented here, the global analytical approach of the problem will be detailed in this section. The overdot notation is used for time derivatives.

As mentioned previously, we will consider only the response of the isolated first stage by computing the inter-strand coupling currents called $J_{k\,k+1}(z)$ (average current density flowing from strand k to $k+1$) and assuming a uniform current distribution along each superconducting shell noted $I_k(z)$. To be able to express the time constant of the system, we assumed an equivalent simplified (rectangle) current distribution between each strand. Using Kirchhoff's current law, we first obtain

$$\frac{d}{dz}I_k(z) = \left(J_{k-1\,k}(z) - J_{k\,k+1}(z)\right)l_c \tag{5}$$

In addition, using Faraday's law of induction, the fact that $\vec{E} = \vec{0}$ along the center of each strand and Ohm's law, we can derive

$$2R\rho_t \frac{d}{dz}J_{k\,k+1}(z) = \frac{d}{dz}\dot{\Phi}_{k\,k+1}(z) \tag{6}$$

with $\Phi_{k\,k+1}(z)$ the magnetic flux enclosed between the centers of strands k and $k+1$ from $z = 0$ to z.

By neglecting the axial component of the magnetic field B_z, we can reduce the magnetic vector potential $\vec{A}$ to its axial component only, therefore $\vec{A} = A_z\vec{e_z}$ and

$$\frac{d}{dz}\Phi_{k\,k+1}(z) = A_{z_{k+1}}(z) - A_{z_k}(z) \tag{7}$$

$A_{z_k}(z)$ is the value of A_z in the center of strand k at z.

Finally, using (5), (6) and (7), we derive for $1 \le k \le N$

$$\frac{d^2}{dz^2}I_k(z) = \frac{l_c}{2R\rho_t}\left(2\dot{A}_{z_k}(z) - \dot{A}_{z_{k-1}}(z) - \dot{A}_{z_{k+1}}(z)\right) \tag{8}$$

A_{z_k} can be expressed as $A_{z_a\,k} + A_{z_r\,k}$ with $A_{z_a\,k} = -x_k B_a$ (x_k is the abscissa of the center of strand k at z) and $A_{z_r\,k}$ the term due to the induced screening currents $(I_k)_{1\le k\le N}$. Since $\dot{B}_a$ is spatially uniform, using (8), we see that $\dot{A}_{z_a\,k}$ induces screening currents of the form $I_k = I_0\cos\left(\theta_k(z)\right)$ with I_0 depending on time only and $\theta_k(z) = 2\pi z/l_p + 2(k-1)\pi/N$. Using this current distribution and the Biot-Savart law for vector potential, we can show that $A_{z_r\,k} = \beta I_0\cos\left(\theta_k(z)\right)$, with β an integral depending on R_c, R_f, l_p and N only. Unfortunately there is no simple analytical expression of β. However, using geometrical considerations on this particular configuration we have noticed that the $A_{z_r\,k}$ value created in the center of strand k at z by the considered current distribution could be accurately approximated by

$$A_{z_r\,k}(z) = \mu_0\gamma_N/(2\pi).I_0\cos\left(\theta_k(z)\right) \tag{9}$$

with, for $N \ge 2$ $\gamma_N = \ln\left(\frac{2R_c}{R_f}\right) -$

$$2\sum_{j=1}^{floor\left(\frac{N-1}{2}\right)}\cos\left(j\frac{2\pi}{N}\right)\ln\left(\sin\left(j\frac{\pi}{N}\right)\right) > 0$$

In order to validate this expression, we have then numerically computed β for many values of N (between 2 and 100) assuming a realistic ratio $2\pi R_c/l_p$ of 0.065 (ratio used in the first cabling stage of JT-60SA TF conductor). The discrepancy between computed β values and $\mu_0\gamma_N/(2\pi)$ analytical values never exceeded 0.1%.

Using the expression given by (9) in (8) enables us to reduce the problem to the following equation on amplitude I_0

$$\begin{cases} I_0 + \tau_2 \dot{I}_0 = \frac{l_c}{\rho_t} \dot{B}_a \left(\frac{l_p}{2\pi}\right)^2 \; for\; N = 2 \\ I_0 + \tau_N \dot{I}_0 = \frac{2l_c}{\rho_t} \dot{B}_a \sin\left(\frac{\pi}{N}\right) \left(\frac{l_p}{2\pi}\right)^2 \; for\; N \geq 3 \end{cases} \quad (10)$$

$$\tau_2 = \frac{\mu_0}{2R\rho_t} \frac{l_c}{\pi} \left(\frac{l_p}{2\pi}\right)^2 \gamma_2, \tau_N = \frac{\mu_0}{R\rho_t} \frac{l_c}{\pi} \left(\frac{l_p}{2\pi}\right)^2 \sin^2\left(\frac{\pi}{N}\right) \gamma_N \; (N \geq 3)$$

The average instant power density $P_{vol}(z)$ dissipated from $z = 0$ to z computed dividing $P = \iiint_V \vec{J}.\vec{E}\, dV$ by the circumscribed volume (see Fig. 1) of the cable $\pi(R_c + R)^2 z$ leads to the expressions (as functions of I_0)

$$\begin{cases} P_{vol}(z) = \frac{\rho_t \pi}{l_c {l_p}^2 R} {I_0}^2 \left[1 - \mathrm{sinc}\left(\frac{4\pi z}{l_p}\right)\right] \; for\; N = 2 \\ P_{vol}(z) = \frac{\rho_t \pi}{l_c {l_p}^2 R} {I_0}^2 \frac{N}{\left[1+\sin\left(\frac{\pi}{N}\right)\right]^2} \; for\; N \geq 3 \end{cases} \quad (11)$$

where $\mathrm{sinc}(x) = \sin(x)/x$.

It is important to notice that the average instant power density dissipated in a doublet (i.e. $N = 2$) depends on z; this is no longer true for a triplet, a quadruplet and so on.

If we now look at equation (10), when the steady state regime for coupling currents is reached, we have $I_0 = \frac{2l_c}{\rho_t} \dot{B}_a \sin\left(\frac{\pi}{N}\right) \left(\frac{l_p}{2\pi}\right)^2$ and $\dot{B}_{int} = \dot{B}_a$. Although the magnetic field inside the N-uplet B_{int} is not uniform, we can represent the N-uplet as a magnetic dipole introducing an equivalent internal uniform magnetic field $B_{int\,eq}$ oriented along the y-axis. In doing so, we just have to replace $\dot{B}_a$ by $\dot{B}_{int\,eq}$ in the expression of I_0 above since $\dot{B}_a$ and $\dot{B}_{int\,eq}$ are both uniform inside the N-uplet. Using this new formulation and after integration in time, equation (10) becomes

$$B_{int\,eq} + \tau_N \dot{B}_{int\,eq} = B_a \quad (12)$$

Continuing the analogy with the dipole, we can use (3), τ_N expressions, (11) and $I_0 = \frac{2l_c}{\rho_t} \dot{B}_{int\,eq} \sin\left(\frac{\pi}{N}\right) \left(\frac{l_p}{2\pi}\right)^2$, to write

$$\begin{cases} nk = \frac{1}{2\gamma_2}\left[1 - \mathrm{sinc}\left(\frac{4\pi z}{l_p}\right)\right] = \frac{1}{2\gamma_2} \; for\; z = l_p, for\; N = 2 \\ nk = \frac{N}{\gamma_N} \frac{1}{\left[1+\sin\left(\frac{\pi}{N}\right)\right]^2} \; for\; N \geq 3 \end{cases} \quad (13)$$

Table 1 displays some values of nk for two R_f (i.e. filamentary zone radius) to R (i.e. strand radius) ratios which are bounding values for most strands. It is also interesting to note that for a large N value (i.e. strands arranged in a circle, as edge filaments in a composite) the nk function approaches 2, which is exactly the value given by (2) for a composite.

TABLE I
TABLE OF NK VALUES FOR SEVERAL VALUES OF N

Ratio R_f/R	NK VALUE					
	$N = 2$	$N = 3$	$N = 4$	$N = 5$	$N = 6$	$N \to \infty$
0.7	0.476	0.821	0.983	1.085	1.163	2.000
0.9	0.626	1.079	1.199	1.258	1.307	2.000

We have now analytically derived the τ and nk values of a single stage that respectively correspond to its time constant and its partial shielding coefficient, and expressed their values as a function of the electrical and geometrical parameters of the N-uplet.

C. *Comparisons with other models*

The purpose of this section is to reinforce the validity of the N-uplet model by comparing its results in extreme time regimes (constant or infinitely fast magnetic excitation).

A previous work [14] has derived the following average instant power density per unit volume of composite $\bar{P}$ in a one stage cable under constant magnetic excitation (i.e. constant $\dot{B}_a$)

$$\bar{P} = \frac{2\Psi R}{\rho_b e_b \pi} {\dot{B}_a}^2 \left(\frac{p_1}{2\pi}\right)^2 \left[1 - \frac{R_f p^*}{R p_1}\right]^2 \quad (14)$$

where p_1 is the twist pitch of the first stage, p^* the effective twist pitch of filaments in the composite, R the composite radius and Ψ the average angular thickness of contacts between two strands (thus $2\Psi R$ is the contact width).

It is then interesting to compare losses expressions (11) and (14). Rescaling losses expression (11) to the volume of composites and using $I_0 = \frac{2l_c}{\rho_t} \dot{B}_a \sin\left(\frac{\pi}{N}\right) \left(\frac{l_p}{2\pi}\right)^2$ leads to

$$\bar{P} = \frac{l_c}{\rho_b e_b \pi} {\dot{B}_a}^2 \left(\frac{l_p}{2\pi}\right)^2 \quad (15)$$

Expression (15) contains losses arising from the shielding by the strand stage which was not considered in our approach. Thus (14) is reduced to $\frac{2\Psi R}{\rho_b e_b \pi} {\dot{B}_a}^2 \left(\frac{p_1}{2\pi}\right)^2$, and since, by definition, $l_c = 2\Psi R$ (contact width) and $l_p = p_1$ (twist pitch of the first stage), we observe the exact same results.

Another relevant comparison, but this time under step function regime, was carried out computing the inductance matrix of the system (i.e. regarding filamentary zones as straight hollow tubes carrying current). The induced currents computed with the inductance matrix and with (10) were exactly the same. Furthermore, we have also simulated the reaction of a group of composites (represented by a hundred edge filaments) to a step function using the inductance matrix approach but this time considering the filaments as straight hollow tubes carrying current. In this case, the effective shielded surface (which corresponds to nkS with S the circumscribed surface) differs from less than 20% with the value computed using (13).

The distribution of current observed among the filaments is of particular interest since it shares obvious similarities with the distribution of current among strands in a two stage cable whose modeling is exposed in the next section.

III. ANALYTICAL MODELING OF TWO STAGES

This model is in the continuity of the N-uplet one, but aims at describing coupling losses generated in a two cabling stage conductor (i.e. N_2 groups of N_1 strands). Once again, the strand scale is ignored, and the model is focused on the dynamics of shielding of the field variation by the two stages. The assumptions remain unchanged and, to simplify the approach, we will consider each group of N_1 strands as a N_1-uplet, thus having the l_{p_1}, l_{c_1}, ρ_{t_1}, R_{c_1}, R_1 parameters corresponding to the l_p, l_c, ρ_t, R_c, R parameters of the N-uplet for $N = N_1$ (see Fig. 1). We then consider this N_1-uplet as an element whose volume is the circumscribed volume of the N_1-

uplet, thus with a radius $R_2 = R_{c_1} + R_1$. The N_2 groups of N_1 strands can then be represented as a N_2-uplet of elements with a twist pitch l_{p_2} and a twisting radius R_{c_2} and its own values of ρ_{t_2} and l_{c_2} parameters. The current flowing in the filamentary zone of strand k_1 of element k_2 is noted $I_{k_1k_2}(z)$ and is split by thought into ${I_{k_1k_2}}^{(1)}$, due to the voltages induced between strands of element k_2, and ${I_{k_1k_2}}^{(2)} = \frac{{I_{k_2}}^{(2)}}{\mathrm{N}_1}$, ${I_{k_2}}^{(2)}$ being due to the voltages induced between the N_2 elements. This notation helps to dissociate the shielding accomplished by the different stages.

Under constant $\dot{B}_a$ regime, the model naturally leads to

$$I_{k_1k_2} = I_{0_1}\cos(\theta_{k_1}) + \frac{I_{0_2}}{\mathrm{N}_1}\cos(\theta_{k_2}) \quad (16)$$

$$\text{with } \begin{cases} \theta_{k_1} = \frac{2\pi z}{l_{p_1}} + \frac{2\pi(k_1-1)}{\mathrm{N}_1}, I_{0_1} = \frac{2l_{c_1}}{\rho_{t_1}}\dot{B}_a \sin\left(\frac{\pi}{N_1}\right)\left(\frac{l_{p_1}}{2\pi}\right)^2 \\ \theta_{k_2} = \frac{2\pi z}{l_{p_2}} + \frac{2\pi(k_2-1)}{\mathrm{N}_2}, I_{0_2} = \frac{2l_{c_2}}{\rho_{t_2}}\dot{B}_a \sin\left(\frac{\pi}{N_2}\right)\left(\frac{l_{p_2}}{2\pi}\right)^2 \end{cases}$$

Expression (16) is a simple superposition of the shielding due to each stage. In these conditions the induced currents are a sum of two cosine functions with spatial periods l_{p_1} and l_{p_2} along the z-axis.

However, while investigating transient regimes the simulated response of this system to a step function using the inductance matrix approach showed clearly that the induced currents are also composed of cosine functions with spatial periods different from l_{p_1} and l_{p_2} whose amplitudes are not negligible. We have therefore refined the model using an approach similar to the N-uplet one and derived the following equations governing the currents flowing in the filamentary zones

$$\begin{cases} c_1\frac{d^2}{dz^2}\left[{I_{k_1k_2}}^{(1)}\right] + M_{1\,1}\left[\dot{I}_{k_1k_2}{}^{(1)}\right] = Y_1\dot{B}_a + M_{1\,2}\left[\dot{I}_{k_2}{}^{(2)}\right] \\ c_2\frac{d^2}{dz^2}\left[{I_{k_2}}^{(2)}\right] + M_{2\,2}\left[\dot{I}_{k_2}{}^{(2)}\right] = Y_2\dot{B}_a + M_{2\,1}\left[\dot{I}_{k_1k_2}{}^{(1)}\right] \end{cases} \quad (17)$$

where $c_1 = \frac{4\pi R_1}{\mu_0}\frac{\rho_{t_1}}{l_{c_1}}$ and $c_2 = \frac{4\pi R_2}{\mu_0}\frac{\rho_{t_2}}{l_{c_2}}$.

$\left[{I_{k_1k_2}}^{(1)}\right]$ and $\left[{I_{k_2}}^{(2)}\right]$ are the column vectors of the ${I_{k_1k_2}}^{(1)}$ and ${I_{k_2}}^{(2)}$ currents, Y_1 and Y_2 are column vectors whose coefficients are $y_{1_{k_1k_2}} = -(8\pi R_1/\mu_0).\sin(\pi/N_1)\cos(\theta_{k_1})$ and $y_{2_{k_2}} = -(8\pi R_2/\mu_0).\sin(\pi/N_2)\cos(\theta_{k_2})$.

To obtain the M matrices, which correspond to nondimensionalized inductive matrices, we have used geometrical considerations (similar to these used in the N-uplet model) and thus have assumed that the $A_{z_{r\,k_1k_2}}(z)$ value inside the center of strand k_1 of element k_2 at z created by the ${I_{k_1k_2}}^{(1)}$ and ${I_{k_2}}^{(2)}$ currents could be approximated by

$$A_{z_{r\,k_1k_2}}(z) = -\frac{\mu_0}{2\pi}\sum_{j_2=1}^{N_2}\sum_{j_1=1}^{N_1} I_{j_1j_2}(z)\ln\left(\frac{d_{j_1j_2k_1k_2}(z)}{R_f}\right) \quad (18)$$

with $d_{j_1j_2k_1k_2}(z)$ the distance between the center of strand k_1 of element k_2 and the center of strand j_1 of element j_2 at z, but taken equal to R_f if $j_1 = k_1$ and $j_2 = k_2$.

Since (18) is an approximation of the real expression of $A_{z_{r\,k_1k_2}}(z)$ as a function of the $I_{k_1k_2}$ currents, we have therefore performed a comparison between the numerically computed values of $A_{z_{r\,k_1k_2}}(z)$ with Biot-Savart law and (18) using several realistic values of the different parameters (save N_1 and N_2 set to 3). We have found out that the discrepancy between the two values never exceeded 5%.

Adapting (8) to the modeling of two stages using simple analogies with the N-uplet model and using (18), it is possible to derive the analytical expressions of the coefficients of the M matrices. However, because of their complicated expressions, only the one of $M_{1\,1}$ (a N_1N_2-by-N_1N_2 matrix) is presented

$$M_{1\,1}(j,k) = \ln\left[\frac{\left(d_{k_1k_2j_1j_2}(z)\right)^2}{d_{k_1k_2j_1-1j_2}(z).d_{k_1k_2j_1+1j_2}(z)}\right] \quad (19)$$

with $k_2 = ceil\left(\frac{k}{N_1}\right)$, $j_2 = ceil\left(\frac{j}{N_1}\right)$, $k_1 = k + N_1(1-k_2)$, $j_1 = j + N_1(1-j_2)$ and $d_{k_1k_2j_1j_2}(z)$ the function defined in (18).

Moreover, the last lines of the two matrix equations (17) being redundant, the zero transport current equations

$$\begin{cases} \forall\, k_2,\ {I_{N_1k_2}}^{(1)} = -\sum_{k_1=1}^{N_1-1} {I_{k_1k_2}}^{(1)} \\ {I_{N_2}}^{(2)} = -\sum_{k_2=1}^{N_2-1} {I_{k_2}}^{(2)} \end{cases} \quad (20)$$

are also needed to complete the systems.

The comparison of the induced currents computed with the inductance matrix and with (17) and (20) for a step function with $N_1 = 3$ and $N_2 = 3$ has shown a good agreement (within the range of 15%) in terms of average current carried by each triplet.

In a near future, we will be able, thanks to this model, to derive the analytical $n\alpha_j$ and Θ_j values (discussed in the introduction) for a two cabling stage conductor before iterating this method to the CICC scale.

IV. Conclusion and Perspectives

We have developed a new analytical modeling describing AC coupling losses generated in a single stage (N-uplet model) for any time regime and represented it as a magnetic dipole by expressing fully analytically its nk and τ values. The nk expression has been validated by its limit for a large number of strands ($N \gg 1$) and the N-uplet model is consistent with a previous analytical modeling [14] for constant $\dot{B}_a$ and is in good agreement with the inductance matrix approach for a step function. We have also derived the equation system governing a two cabling stage conductor and assessed its inductive part thanks to a comparison with a purely inductive model under step function regime; its resistive part is strongly advanced and will be finalized numerically and/or experimentally.

Furthermore, the future work will focus on the analytical improvement of our model, first, by the incorporation of the strand stage, and second, by the analytical derivation of the $n\alpha_j$ and Θ_j values, which for now, are experimentally adjusted in the MPAS model. This work will be supplemented with experimental comparisons, and, since our model considers ideal strand trajectories, with its adaptation on a more realistic architecture (real strand trajectories) extracted from a non-destructive analysis of a CICC via X-ray tomography [15].

REFERENCES

[1] G. Ries, *AC-losses in multifilamentary superconductors at technical frequencies*, I.E.E.E. Trans. on Magnetics, MAG-13, No. 1, January 1977, pp. 524–526.

[2] A.M. Campbell, *A general treatment of losses in multifilamentary superconductors*. Cryogenics, Vol. 22, 1982, pp. 3-16.

[3] JP Soubeyrand, B. Turck, *Losses in superconducting composites under high rate pulsed field*, I.E.E.E. Trans. on Magnetics, Vol. 15, January 1979, pp. 248–251.

[4] M. N. Wilson, "Time-vaying fields and A.C. losses" in *Superconducting Magnets,* New York: Oxford University Press Inc., 1983, pp. 176–180.

[5] P. Tixador, "Supraconductivité" in *Les supraconducteurs,* Paris, France: Editions Hermès, 1995, pp. 53–58.

[6] B. Turck, L. Zani, *A macroscopic model for coupling current losses in cables made of multistages of superconducting strands and its experimental validation.* Cryogenics, Vol. 50, 2010, pp. 443-449.

[7] A. Nijhuis, HHJ. ten Kate, PL. Bruzzone, L. Bottura, *Parametric study on coupling loss in subsize Iter Nb3Sn Cabled Specimens*, I.E.E.E. Trans. on Magnetics, Vol. 32, July 1996, pp. 2743–2746.

[8] HHJ. ten Kate, *AC losses and magnet research*, Advances in Cryogenic Engineering, Vol. 40, 1994, pp. 559–568.

[9] A. Nijhuis, HHJ. ten Kate, JL. Duchateau, PL. Bruzzone, *Coupling loss time constant in full size Nb3Sn CIC model conductors for fusion magnets*, Advances in Cryogenic Engineering, Vol. 42B, 1996, pp. 1281–1288.

[10] PL. Bruzzone, A. Nijhuis, HHJ. ten Kate, *Contact resistance and coupling loss in cable-in-conduit of Cr plated Nb3Sn strands*, Proc. MT-15, Beijing, October 1997. Science Press; 1998. pp. 1295–1298.

[11] A. Nijhuis, Ilyin Yu, W. Abbas, B. ten Haken, HHJ. ten Kate, *Change of interstrand contact resistance and coupling loss in various ITER NbTi conductors with the transverse loading in the Twente Cryogenic Cable Press up to 40,000 cycles*, Cryogenics, Vol. 44, 2004, pp. 319–339.

[12] S. Lelekhov, *A physical model and numerical method for losses investigation in superconducting cable-in-conduit conductors (CICC)*, Cryogenics, Vol. 46, 2006, pp. 1-8.

[13] PL. Bruzzone, *Superconductivity: hysteresis and coupling losses*, Lee Peter J, editor, Engineering superconductivity, Wiley-Interscience, 2001, pp. 138–152.

[14] T. Schild, D. Ciazynski, *A model for calculating AC losses in multistage superconducting cables*, Cryogenics, Vol. 36, 1996, pp. 1039-1049.

[15] I. Tiseanu, L. Zani, C. Tiseanu, T. Craciunescu, C. Dobrea, *Accurate 3D modeling of Cable in Conduit Conductor type superconductors by X-ray microtomography*, Fusion Engineering and Design, Vol. 98–99, 2015, pp. 1176-1180